Supplemental Information:

Endothelial Hypoxia Inducible Factor-2alpha (HIF-2α) regulates murine pathological angiogenesis and revascularization processes

Nicolas Skuli[1,2], Amar J. Majmundar[2,3], Bryan L. Krock[2], Rickson C. Mesquita[4], Lijoy K. Mathew[1,2], Zachary L. Quinn[1,2], Anja Runge[1,2,5], Liping Liu[1,2,6], Meeri N. Kim[4], Jiaming Liang[4], Steven Schenkel[4], Arjun G. Yodh[4], Brian Keith[1,7], M. Celeste Simon[1,2,8]

[1]Howard Hughes Medical Institute, [2]Abramson Family Cancer Research Institute, [3]School of Medicine, [4]Department of Physics & Astronomy, [7]Department of Cancer Biology, [8]Department of Cell and Developmental Biology, University of Pennsylvania, Philadelphia, PA 19104, USA.

Present Affiliation and location:

[5]Division of Vascular Oncology and Metastasis, German Cancer Research Center, Heidelberg, D-69120, Germany.

[6]Merck Research Laboratories, West Point, PA 19486, USA.

Corresponding author:

M. Celeste Simon, PhD
Scientific Director and Investigator, Abramson Family Cancer Research Institute
Investigator, Howard Hughes Medical Institute
Professor, Cell and Developmental Biology
University of Pennsylvania School of Medicine
456 BRB II/III, 421 Curie Boulevard
Philadelphia, PA 19104-6160

Telephone number: 215-746-5532
Fax number: 215-746-5511
E-mail: celeste2@mail.med.upenn.edu

Conflict of interest: The authors declare no competing financial interests

Supplemental Information:

Methods

Antibodies

Antibodies were purchased from commercial sources and used according to manufacturers' instructions. Specifically: CD31 (Clone MEC13.3), ICAM-2, biotin-CD31, biotin-ICAM-2, Fc Block (BD Pharmingen) ; Von Willebrand factor (Millipore) ; Actin, Dll4, Ang2, NICD, Desmin (Abcam) ; Ang2 (Santa Cruz) ; smooth muscle actin (clone 1A4), FITC-smooth muscle actin (Sigma) ; HIF-1α (Transduction Labs and Novus) and HIF-2α (Novus) ; Ki67 (BD Biosciences) ; Horseradish peroxidase-labeled goat anti-rabbit IgG or anti-mouse IgG (Cell signaling). Alexa 488/546 conjugated anti-mouse, rabbit, and goat IgG were purchased from Invitrogen.

Speckle imaging, blood flow and oxygenation assessment

DCS measurements were performed with a home-built instrument containing two continuous wave, long coherent 785 nm lasers (CrystaLaser Inc., Reno, NV) and eight avalanche photodiodes (PerkinElmer, Canada). Two 4-channel autocorrelator boards (Correlator.com, Bridgewater, NJ) were employed to compute the intensity temporal correlation function for an integration time of 500 ms. Data were collected simultaneously in both limbs, with four detectors distributed symmetrically along one single source positioned at the center, thus providing two source-detector separations (0.5 and 1.0 cm) from both the top and bottom of the source position. Measurements of DCS were also compared with blood flow measurements with a 1-channel LDF (BPM 403A, TSI Inc., St. Paul, MN). In order to compare flow from the same region over the two different techniques, we measured 3 different points along the bottom portion of the DCS probe, symmetrically positioned in each limb.

The DRS system was composed of a 250 W tungsten-halogen light source (TS-428, PI Acton, MA), a spectrometer (SP-150, Acton Research, MA), and a 16-bit, back-illuminated CCD camera (PIXIS:400BR, Princeton Instruments, NJ). The optical probe consisted of a single source and ten detection fibers spaced non-uniformly (0.6, 1.2, 1.8, 2.4, 3, 4, 5, 6, 8, and 10 mm). A

nonlinear fitting procedure was employed to simultaneously fit all data in the optimal wavelength range (600 – 850 nm) using the analytical solution of the photon diffusion equation for a semi-infinite medium with extrapolated zero boundary conditions. For each limb measurement, we collected data at 3 different locations along the limb, and 10 different frames at every location, with an exposure time of 100 ms each.

All DCS, LDF and DRS measurements were performed prior to left hindlimb artery occlusion, in random order. The same set of measurements was repeated right after surgery, and subsequently once a week, up to maximum of four weeks, when the animals were sacrificed.

Quantitative real-time PCR analysis

Applied Biosystem Primer references:

Dll4: Mm00444619_m1 (RefSeq: NM_019454.3)

Hey1: Mm00468865_m1 (RefSeq: NM_010423.2)

Hey2: Mm00469280_m1 (RefSeq: NM_013904.1)

Hes1: Mm00468601_m1 (RefSeq: NM_008235.2)

Hes2: Mm00456108_g1 (RefSeq: NM_008236.4)

Notch1: Mm00435245_m1 (RefSeq: NM_008714.3)

ADM1: Mm00437438_g1 (RefSeq: NM_009627.1)

Tie2: Mm00443254_m1 (RefSeq: NM_013690.2)

Ang1: Mm00456503_m1 (RefSeq: NM_009640.3)

Ang2: Mm00545822_m1 (RefSeq: NM_007426.3)

EphrinB2: Mm01215897_m1 (RefSeq: NM_010111.5)

EphrinB4: Mm01201157_m1 (RefSeq: NM_001159571.1)

VEGF: Mm01281449_m1 (RefSeq: NM_001025250.3)

Immunoblotting

Endothelial cells were incubated under normoxia (21% O_2) or hypoxia (0.5% O_2) for 16 hrs. Cells were harvested and lysed in RIPA buffer. 40 to 80 μg of proteins was loaded on 8% acrylamide gels. After completing SDS-PAGE and electrophoretic transfer for 4 hrs at 4°C,

membranes were blocked for 1 hr in 5% Non Fat Dry Milk (BD Pharmingen) in TBS with 0.05% tween-20 (Sigma). Blots were probed overnight at 4°C with the appropriate antibody and following the manufacturers' instructions. Horseradish peroxidase-labeled goat anti-rabbit IgG or anti-mouse IgG (Cell Signaling) were used, respectively, at 1:10,000 and 1:5,000.

Flow cytometry

Control and KO endothelial cells were prepared as a single cell suspension and washed in FACS buffer (PBS, 5% FCS, 0.5% BSA). Cells were blocked for 10 min using a blocking antibody (Fc Block, BD Pharmingen) in FACS buffer and stained using primary antibodies (CD31, ICAM2 and VWF) for 45 min at 4°C. After washes, cells were incubated with the appropriate secondary antibodies for 30 min at 4°C. Finally, cells were washed twice, resuspended in 500 μl of isotone (Coulter Electronics) and analyzed using BD FACS Calibur system, Flowjo software (Tree Star Inc) and controls with isotype-matched IgG.

Endothelial cells with HIF-1α/HIF-2α acute deletion (Cnt.H1.2/KO.H1.2 and Cnt.H2.2/KO.H2.2)

Lungs from *Hif-2α*$^{fl/\Delta}$ / *Ubc-CreER* and *Hif-1α*$^{fl/fl}$ / *Ubc-CreER* mice were isolated and processed as described above to obtain endothelial cells. This Cre-ER transgene is expressed from the human *Ubiquitin C* promoter encoding the Cre protein fused to a modified form of the estrogen receptor that specifically binds Tamoxifen with high affinity and is inactive until Tamoxifen is administered to the cells (Rusankina et al., 2007, *Cell Stem Cell* 1:113-26). Cre-ER recombinase was activated in cells by adding Tamoxifen (1μM, MP Biomedicals) in culture media. DNA extracted from cells shows that recombination is highly efficient.

Phalloidin Staining

Control and KO cells were rinsed in PBS briefly to remove media components and fixed in 1% paraformaldehyde in PBS (freshly prepared) for 15 min at RT. Aldehyde excess was quenched with 10 mM ethanolamine in PBS for 5 min. Cells were permeabilized in 0.1% Triton-

X100 in PBS for 1 min and incubated in FITC-phalloidin (Molecular Probes) diluted 1:100 in PBS for 15 min. Finally, cells were rinsed 3 times in PBS, 5 min/wash and mounted for microscopy.

Cell proliferation assay

Control and KO cells were seeded into 6 cm dishes at $5x10^4$ cells per well and incubated at 21% O_2 or 0.5% O_2 for 5 days. Every day, cells were harvested, washed in PBS and counted using a hemocytometer.

BrdU and cell death assay

Control and KO cells were pulsed with BrdU (10μM) for 30 minutes. The cells were processed for FACS analysis according to manufacturer's instructions (BD Biosciences). To analyze the percent of cells undergoing cell death, FACS analysis was performed using Annexin V-FITC and PI staining (BD Biosciences).

Invasion assay

Cells were plated in serum-free EGM media (Lonza) on 24-well Transwell inserts (Costar, Corning). The lower chamber contained complete EGM media; after incubation for 8 hrs at 37 °C/5% CO_2/21% O_2 or 0.5% O_2, the inserts were fixed with 3.7% paraformaldehyde/phosphate-buffered saline and stained with 2% crystal violet. The number of invaded cells per 100X field was determined using a Leica 500 microscope (Leica).

Viability assay

We assessed the percentage of viable Cnt. and KO cells in different culture conditions (+/- O_2 and +/- serum). A $1x10^6$ cells/ml cell suspension was prepared and diluted using 1:1 ratio of 0.4% trypan blue solution (Cellgro). Stained cells and total number of cells were determined by hemocytometer counting. The calculated percentage of unstained cells represent the percentage of viable cells.

Collagen adhesion assay

Adhesion assays were performed as described (52). Briefly, KO and related Cnt. ECs were seeded into 24-well plates coated or not with Collagen (1 μg/ml, Upstate) and incubated for 1hr at 37°C under normoxic or hypoxic conditions. Cells were then carefully washed 3 times with PBS, fixed and counted. The number of adherent cells was counted in 6 representative HPFs (high power fields) using an Olympus IX81 microscope (Olympus). The data are representative of three independent experiments.

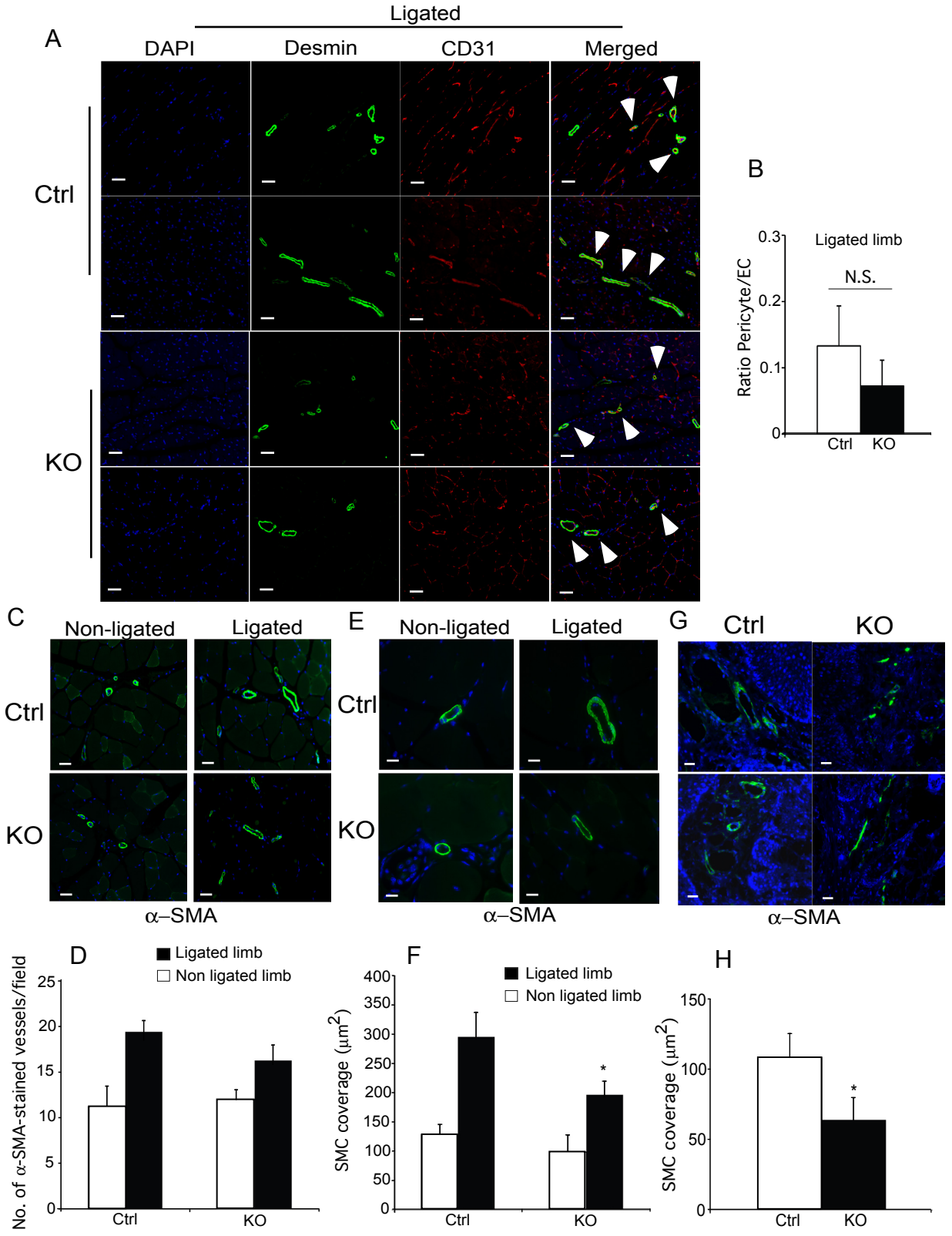

Supplemental Figure 1. Defective smooth muscle cell coverage in mice with endothelial specific HIF-2α deletion. (A) Images showing desmin (pericyte marker) and CD31 (endothelial cell marker) co-staining in ligated limb from Ctrl and KO mice. Scale bars: 40 μm. Magnification 200X. **(B)** Pericyte recruitment is expressed as the ratio between pericyte to EC and no significant (N.S.) difference is observed between Ctrl and KO mice. (Ctrl n=8, KO n=9). **(C)** Pictures showing SMC staining in adductor muscle for ligated and non ligated limb in Ctrl and KO mice. Scale bars: 40 μm. Magnification 200X. **(D)** Quantification of number of α-SMA-stained vessels per field showing no significant difference between Ctrl and KO mice. **(E-F)** In correlation with collateral artery thickness wall reduction, defective smooth muscle cell coverage was observed in KO mice. Representative pictures (E) showing SMC staining in adductor muscle for ligated and non ligated limb in Ctrl and KO mice. SMC coverage per vessel area was assessed (F). Scale bars: 20 μm. Magnification 400X. (Ctrl n=8, KO n=9). **(G-H)** Images showing SMC staining (G) in skin tumors from Ctrl and KO mice. SMC coverage per vessel area was assessed (H). Scale bars: 20 μm. Magnification 400X. (Ctrl n=10, KO n=11). Data are means ± SEM. *P<0.05.

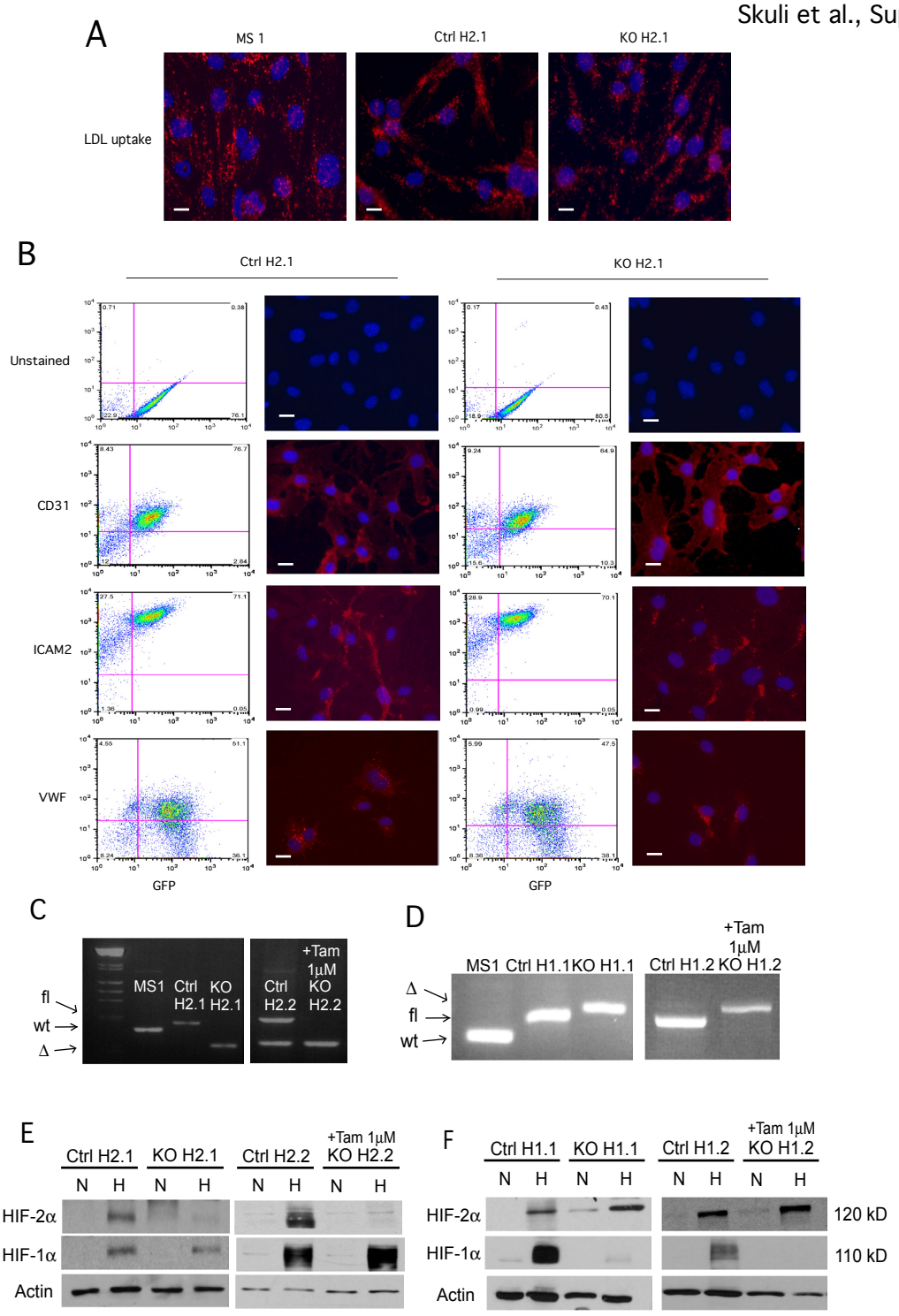

Supplemental Figure 2. Characterization of HIF-1α and HIF-2α KO endothelial cells. (A) Fluorescent immunostaining for acetylated-LDL uptake was studied using MS1, a murine pancreatic endothelial cell line, Ctrl and KO lung endothelial cells. **(B)** Fluorescent immunostaining (right panels) and flow cytometric analyses (left panels) were perfomed for CD31, ICAM2 and von Willebrand Factor using Ctrl and KO lung endothelial cells. Scale bars: 5 μm. Magnification 400X. **(C-D)** PCR reactions showing the efficient recombination in the HIF-1α and HIF-2α KO endothelial cells. **(E-F)** Western blot analysis of HIF-1α and HIF-2α protein expression in Ctrl and KO endothelial cells subjected to 21% (N) or 0.5% (H) O_2 for 6 hrs. The bands appear diffuse due to phosphorylation and other post-translational modifications. Experiments were performed in triplicates.

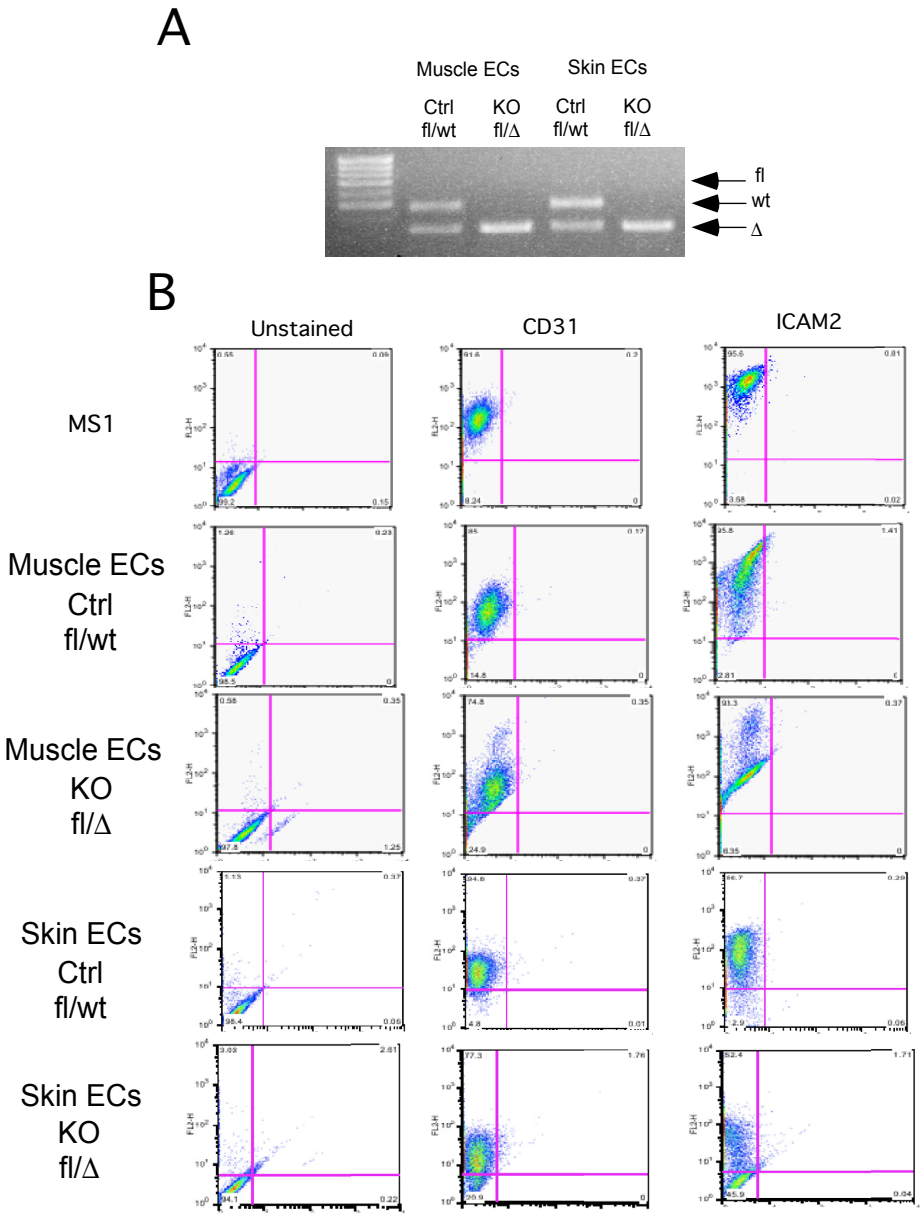

Supplemental Figure 3. Characterization of skin and muscle HIF-2α KO endothelial cells. (A) PCR reactions showing the efficient recombination of the floxed allele in skin and muscle HIF-2α KO endothelial cells. Endothelial cells were isolated from Ctrl (VE-Cad Cre ; HIF-2α fl/wt) and KO (VE-Cad Cre ; HIF-2α fl/Δ) mice. **(B)** Flow cytometric analyses were perfomed for CD31 and ICAM2 using Ctrl and KO skin and muscle endothelial cells.

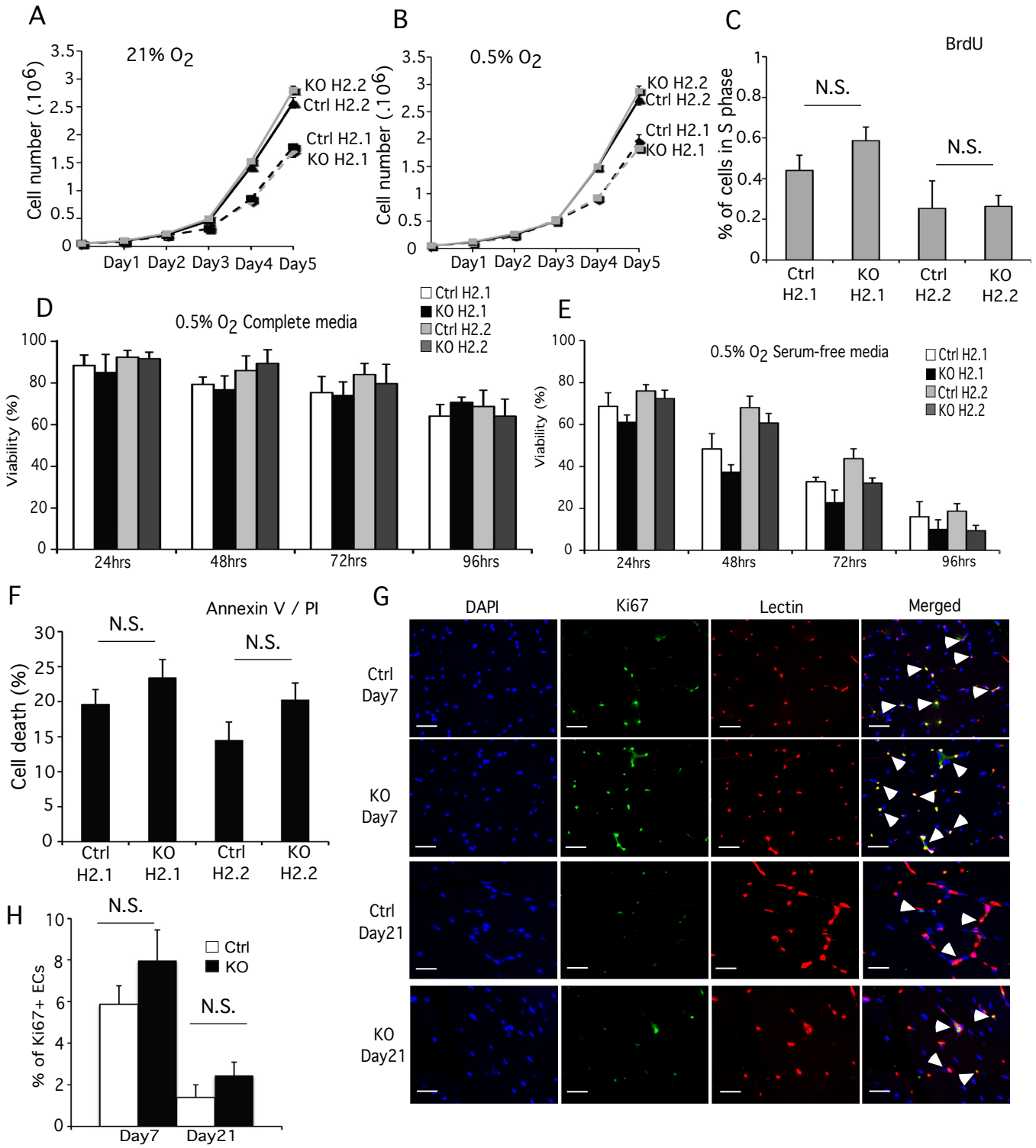

Supplemental Figure 4. HIF-2α deletion does not affect endothelial cell proliferation or viability. (A-B) Ctrl and KO lung ECs were incubated under 21%(A) or 0.5%(B) O_2 in regular culture media and harvested every 24 hrs until the cultures reached confluence. The average cell number of triplicate plates for each condition was determined by counting by hemocytometer following trypsinization. **(C)** Ctrl and HIF-2α KO ECs were incubated under 0.5%O_2 in serum-free media for 48 hrs. Cell cycle was analyzed using BrdU assay. Graph representing the percentage of Ctrl and HIF-2α KO ECs in S after 48hrs under hypoxic conditions (0.5%O_2) in serum-free media. No significant difference in the percentage of ECs in S phase between Ctrl and KO was observed. **(D-E)** Ctrl and KO ECs were cultured at 0.5%O_2 in the presence (D) or absence (E) of serum and viable cells were counted at indicated times. Graphs represent the percentage of viable cell obtained from the average of three independent experiments. HIF-2α KO ECs in serum-free media show a non-statistically significant reduction in viability compared to Ctrl ECs. **(F)** Ctrl and KO ECs were incubated under 0.5%O_2 in serum-free media for 48hrs. Cell death was analyzed using AnnexinV/PI assay. Graph representing the percentage of cell death for Ctrl and KO ECs. No significant difference in cell death between Ctrl and KO ECs was observed. **(G-H)** Proliferation of ECs was assessed *in vivo* at day 7 and day 21 after femoral artery ligation for Ctrl and KO mice using Ki67 and Rhodamine lectin co-staining. (G) Images of Ki67 and Rhodamine lectin co-staining showing increased EC proliferation at day 7 compared to day 21 in adductor muscle, but no significant difference between Ctrl and KO mice. Arrowheads indicate Ki67 positive ECs. Scale bars:20μm. Magnification400X. (H) Quantification of the percentage of Ki67 positive ECs at day 7 and day 21 after femoral artery ligation for Ctrl and KO mice showing no significant difference in EC proliferation *in vivo* between Ctrl and KO mice. (Ctrl n=8, KO n=9). Data are means ± SEM.

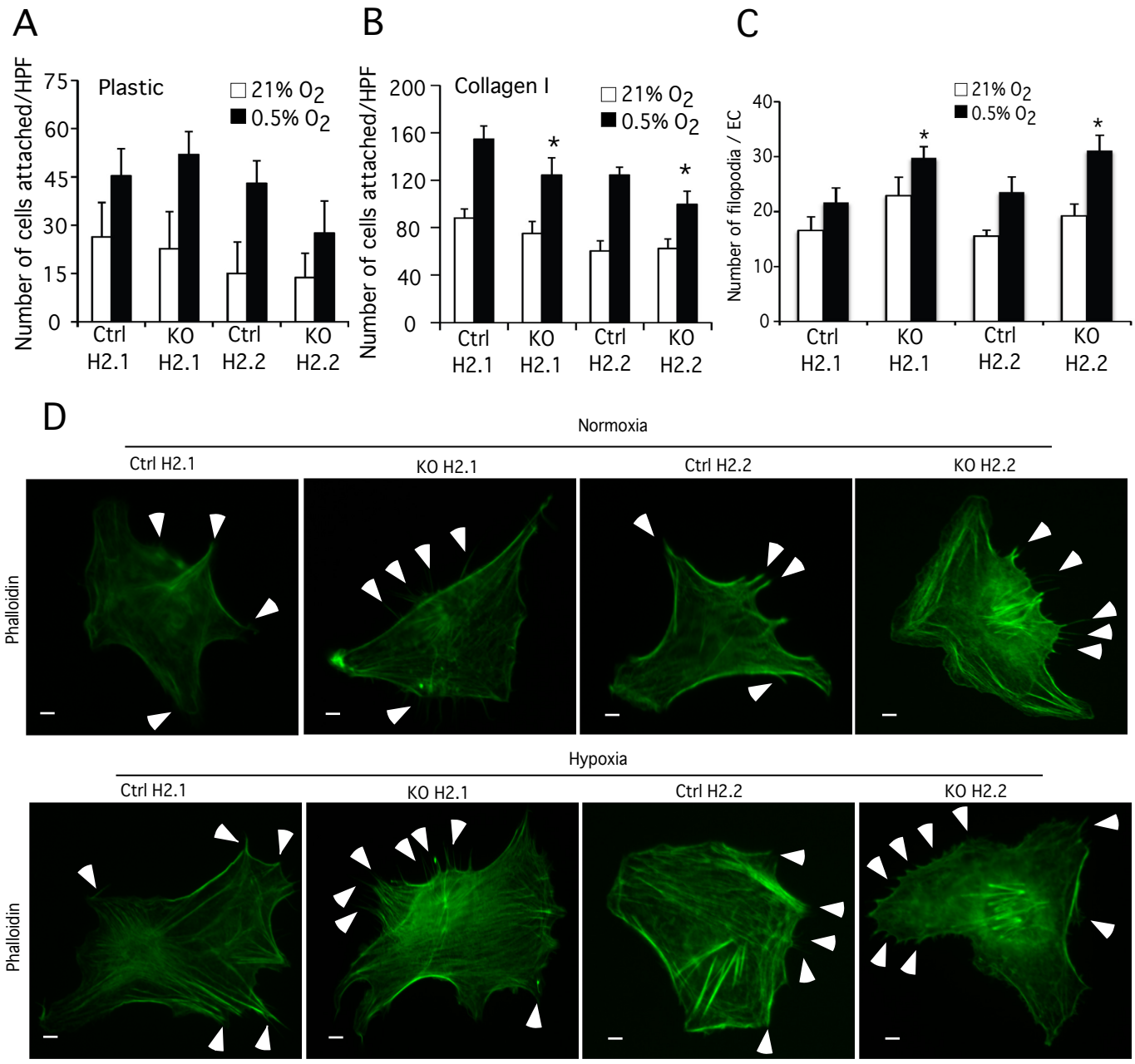

Supplemental Figure 5. HIF-2α deletion affects endothelial cell adhesion and filopodia formation. (A-B) Reduced adhesion of independently derived KO EC lines to plastic (A) or collagen type I- (B) coated plates, under normoxic (21% O_2) or hypoxic (0.5% O_2) conditions, compared to related control EC lines. Cells in 6 random high power fields (HPF) were counted, and combined results from 3 separate experiments are shown. **(C-D)** Number of filopodia was assessed using phalloidin staining. (C) Number of filopodia per EC was quantified and graph shows increased number of filopodia per EC under hypoxic conditions for KO ECs compared to Ctrl. (D) Representative pictures of phalloidin staining performed on Ctrl and KO ECs under normoxic (21% O_2) or hypoxic (0.5% O_2) conditions. Data are means ± SEM. *P<0.05.

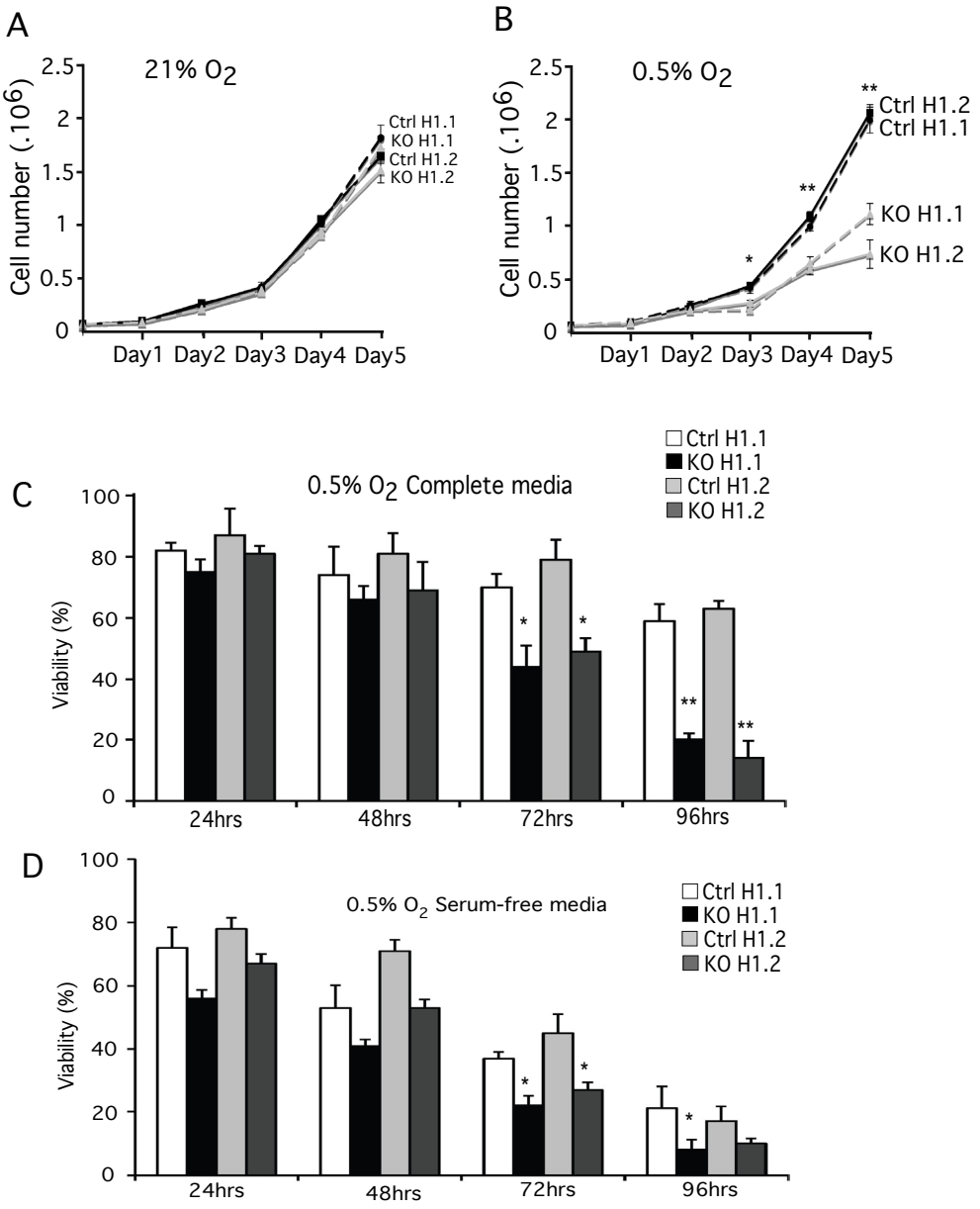

Supplemental Figure 6. HIF-1α deletion affects endothelial cell proliferation and viability. (A-B) Ctrl and HIF-1α KO lung ECs were incubated under 21% (A) or 0.5% (B) O_2 in regular culture media and harvested every 24hrs until the cultures reached confluence. The average cell number of triplicate plates for each condition was determined by counting by hemocytometer following trypsinization. **(C-D)** Ctrl and HIF-1α KO ECs were cultured at 0.5% O_2 in the presence (C) or absence (D) of serum and viable cells were counted at indicated times. Graphs represent the percentage of viable cell obtained from the average of three independent experiments. Data are means ± SEM. *P<0.05 and **P<0.01.

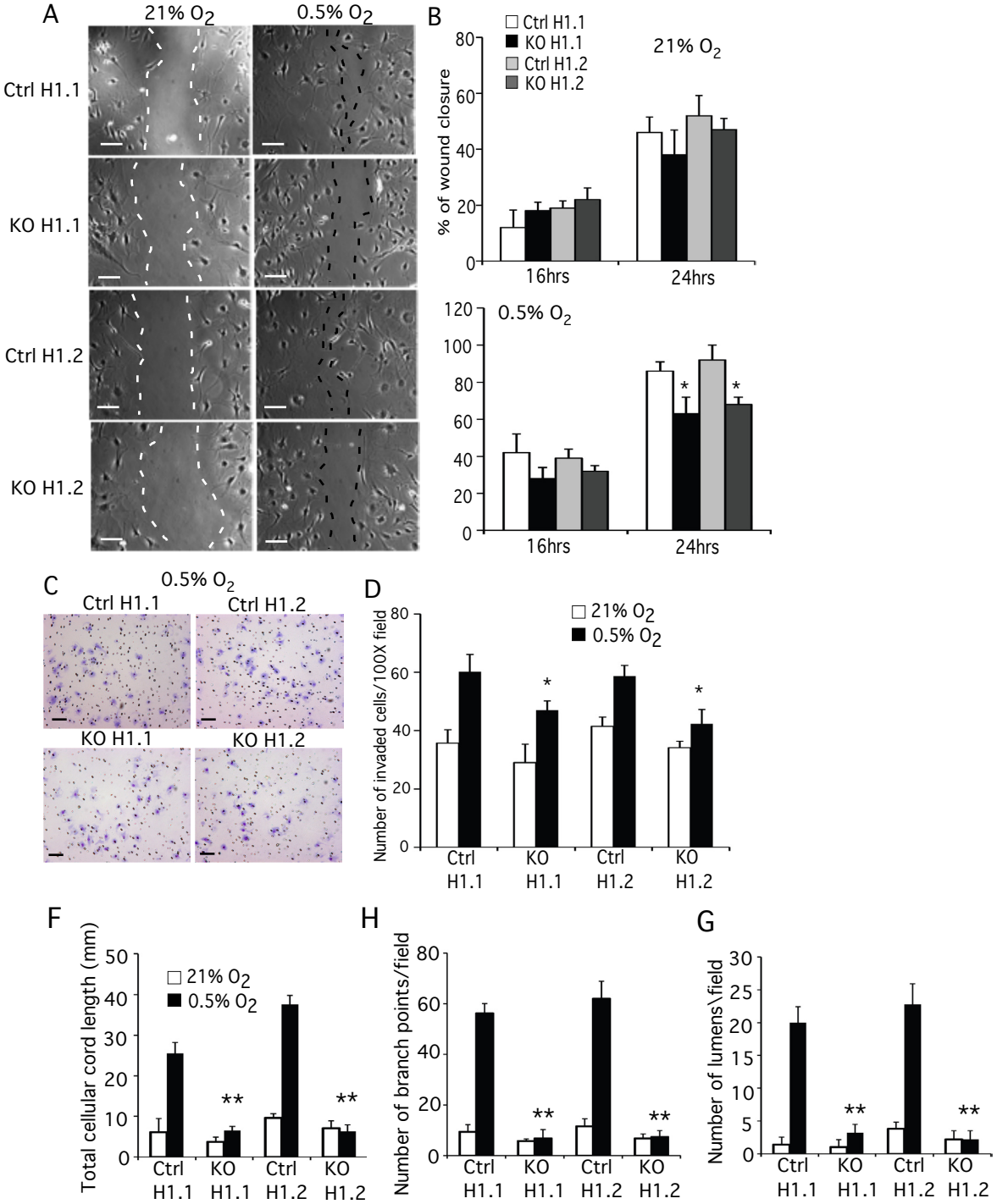

Supplemental Figure 7. HIF-1α deletion affects endothelial cell network formation and migration. (A) Migration of Ctrl and HIF-1α KO lung ECs was assessed under normoxic (21% O_2) or hypoxic (0.5% O_2) conditions at several time points using a scratch wound assay. Representative photographs shown in (A) were taken 24 hrs after scratch. **(B)** Percentage of wound closure was determined and was significantly decreased for HIF-1α KO ECs compared to the control cells at 24 hrs after scratch and under hypoxic (0.5% O_2) conditions. **(C)** EC invasion was further assessed using a Boyden's chamber assay. Photographs represent Ctrl and HIF-1α KO EC invasion after 8 hrs under hypoxic (0.5% O_2) conditions. **(D)** Number of invaded cells was quantified at 8 hrs under normoxic (21% O_2) or hypoxic (0.5% O_2) conditions. Graphs show decreased invasion for HIF-1α KO ECs compared to control cells at 0.5% O_2. **(E)** EC network/capillary formation was assessed using a Matrigel assay. Photographs represent Ctrl and HIF-1α KO EC capillary formation after 8 hrs under normoxic (21% O_2) or hypoxic (0.5% O_2) conditions. **(F-H)** Quantifications of EC network formation reveal significant decrease in total cellular cord length and number of lumens and branch points for HIF-1α KO ECs compared to control cells at 0.5% O_2. Magnification X100. Scale bars: 100 μm. Experiments were performed in triplicates. Data are means ± SEM. *P<0.05, **P<0.01.

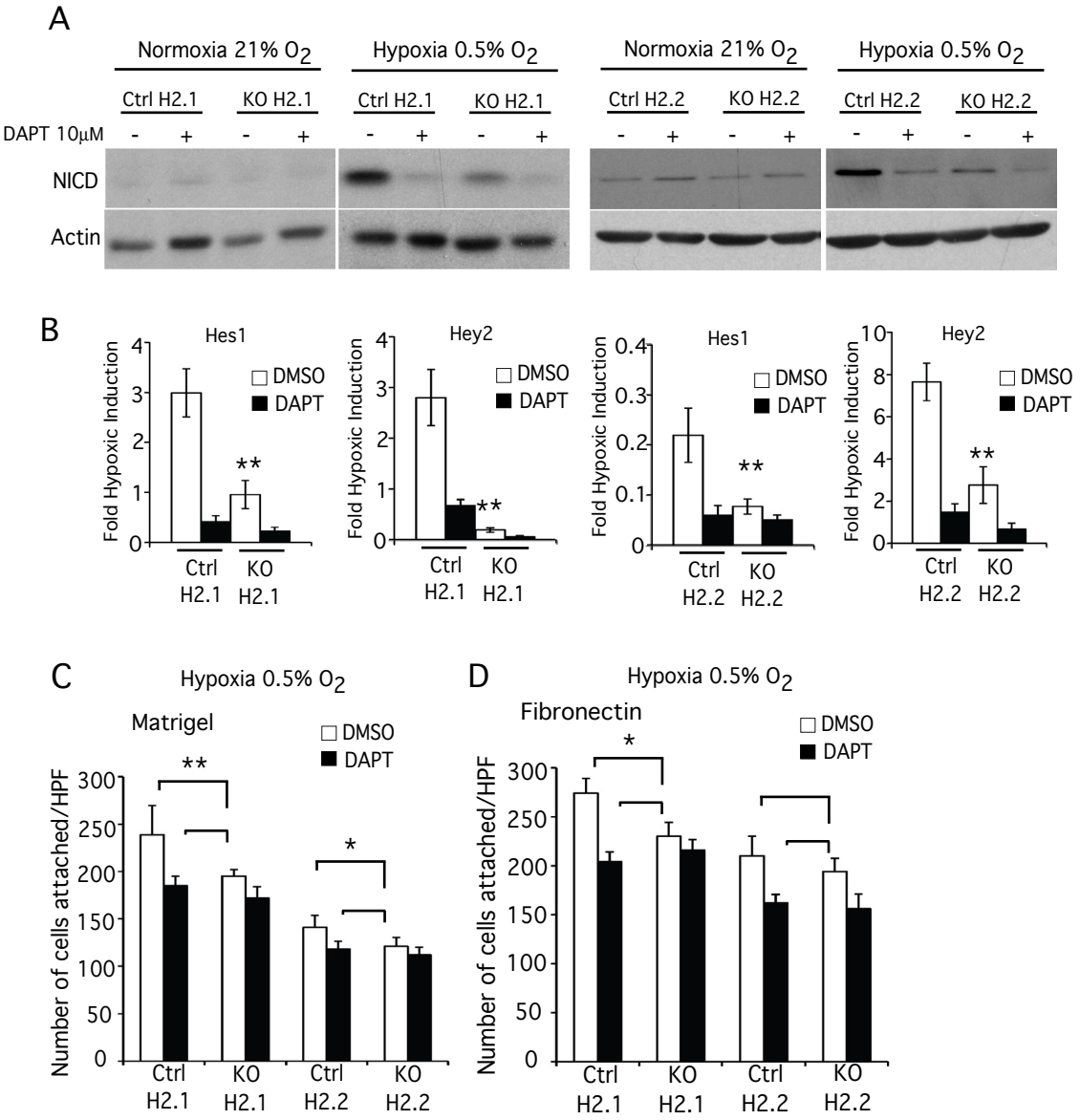

Supplemental Figure 8. Notch pathway inhibition phenocopies HIF-2α deficiency in endothelial cell adhesion. (A) Western blot analysis of Notch Intracellular Domain (NICD) protein expression in Ctrl and KO ECs subjected to 21% (Normoxia) or 0.5% (Hypoxia) O_2 for 6 hrs and treated or not with a Dll4/Notch pathway inhibitor (DAPT). **(B)** Hypoxic induction of Dll4/Notch pathway target gene expression was assessed by qRT-PCR in Ctrl and KO lung ECs treated with DAPT. The relative ratio of hypoxic to normoxic gene expression (fold hypoxic induction) is shown for control and KO ECs. **(C-D)** EC adhesion was assessed using Matrigel and Fibronectin adhesion assays. Quantifications of EC adhesion reveal no significant difference in Matrigel (D) or Fibronectin (E) adhesion between untreated KO ECs and DAPT-treated control cells at 0.5% O_2. Experiments were performed in triplicates. Data are means ± SEM. *P<0.05, **P<0.01.

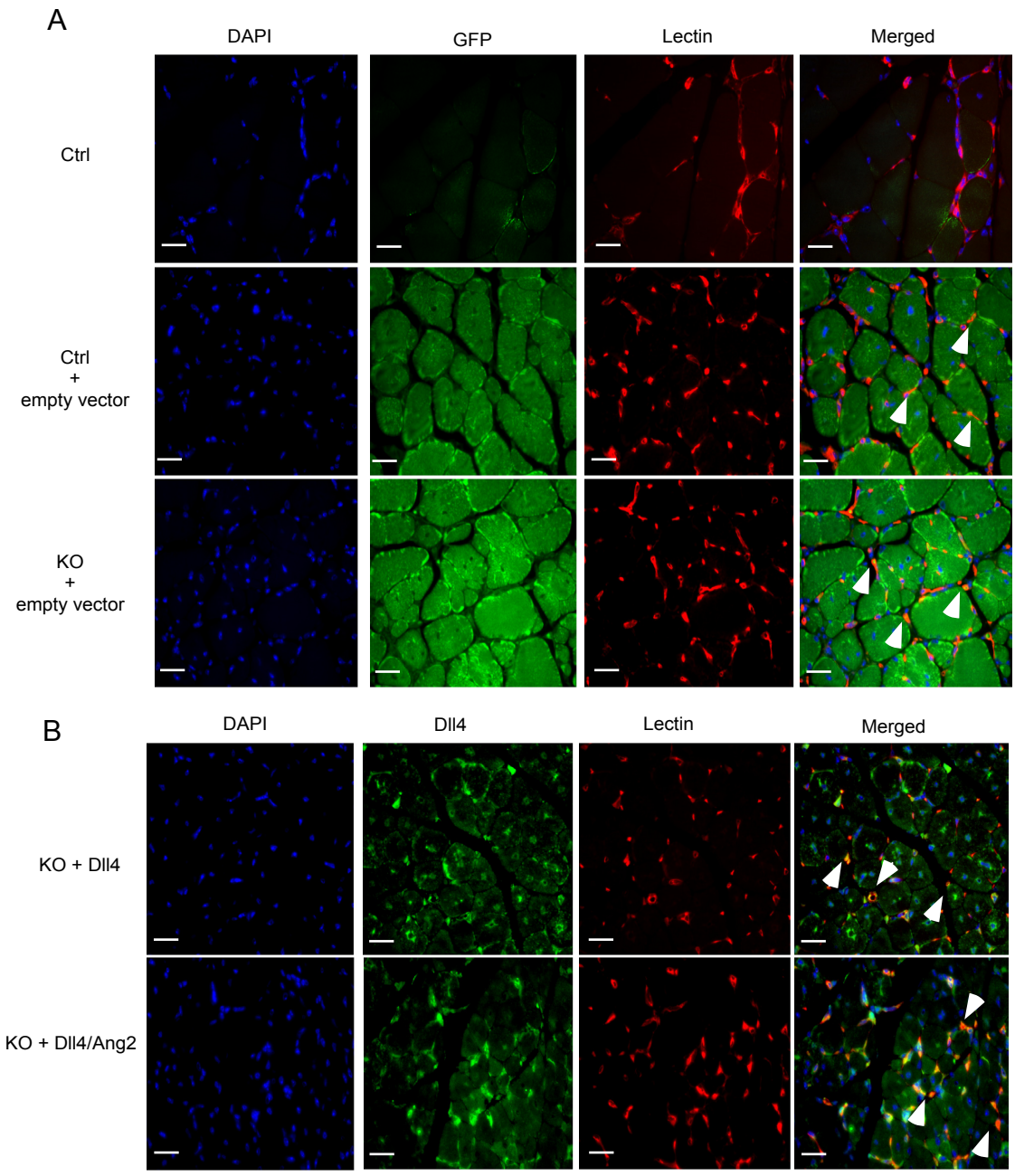

Figure 9. Dll4 and Dll4/Ang2 are sufficient to reverse endothelial HIF-2α deletion phenotypes in a hindlimb ischemia model. (A-B) GFP and Dll4 expression were assessed in adductor of Ctrl and KO mice after intramuscular injection of an empty viral vector (expressing GFP), a viral vector expressing Dll4 or Dll4 vector in combination with intravenous Ang2. (A) Representative images showing GFP expression in muscle fibers and ECs stained with Rhodamine lectin. Arrowheads show ECs expressing GFP. (B) Representative images showing Dll4 expression in muscle fibers and endothelial cells stained with Rhodamine lectin. Arrowheads show ECs expressing Dll4. Please note that the differences in GFP and Dll4 expression patterns, particularly in muscle fibers, may be due to the variable efficiency of the viral vector to express either GFP or Dll4 in this tissue and the detection methods. Scale bars: 20 μm. Magnification 400X. (Ctrl n=20, KO n=20).

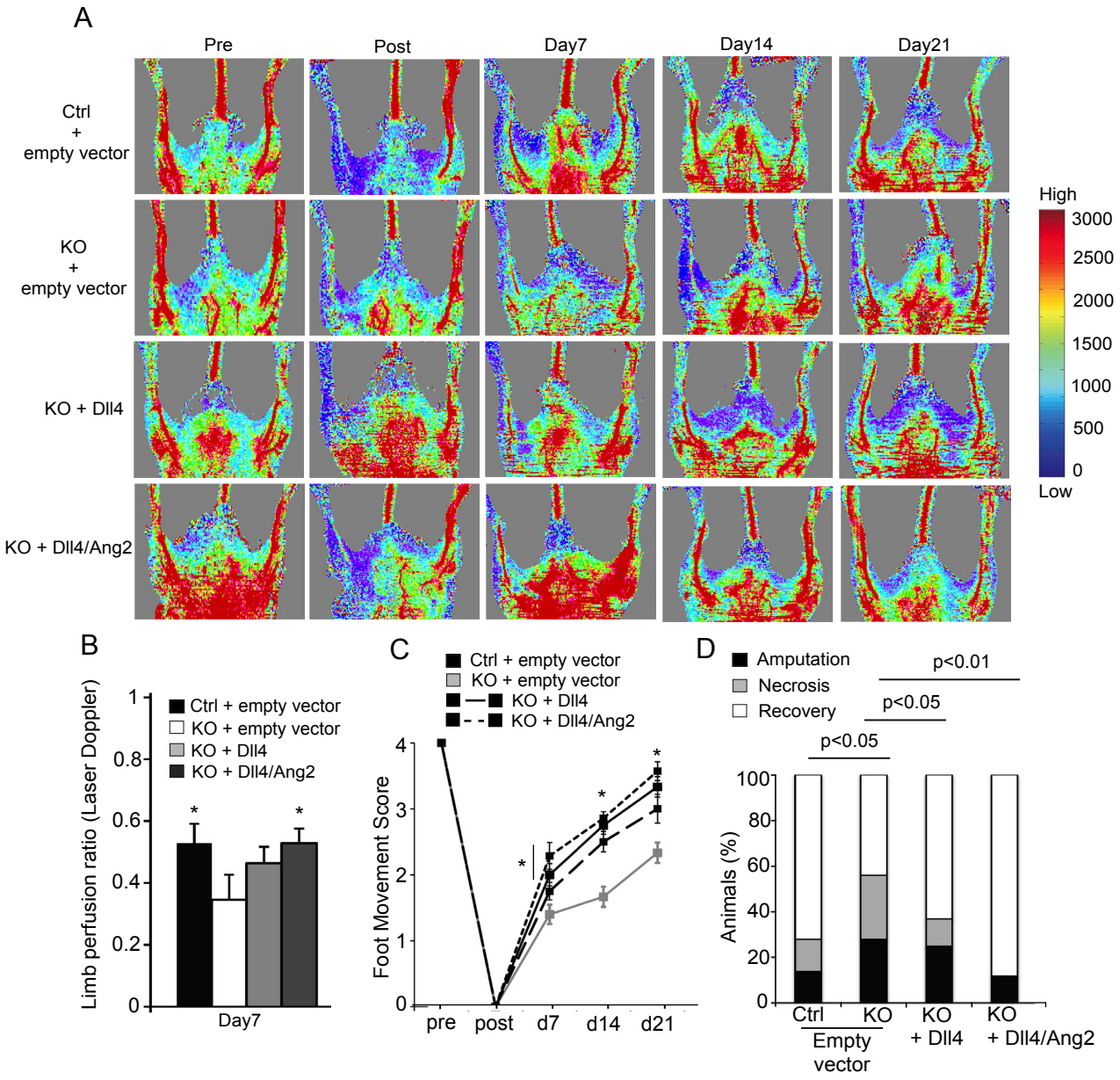

Figure 10. Dll4 and Dll4/Ang2 are sufficient to reverse endothelial HIF-2α deletion phenotypes in a hindlimb ischemia model. Blood flow, foot movement score and necrosis were assessed for Ctrl and KO mice after femoral artery ligation and intramuscular injection of an empty viral vector, a viral vector expressing Dll4 or Dll4 vector in combination with intravenous Ang2. Blood flow was quantified by laser Doppler. **(A-B)** Representative images (A) obtained by laser Doppler showing the efficiency of the surgery distally to the occlusion side and the progressive blood flow recovery after 21 days for Ctrl and KO mice. (B) Quantitative laser Doppler analysis showing the left-to-right limb ratio after occlusion of the femoral artery at day 7. KO mice display a delayed restoration in perfusion compared to Ctrl mice. However, flow is completely restored for mice injected with a viral vector expressing Dll4 or Dll4 vector in combination with Ang2. **(C)** Foot movement was determined and scored between 0 and 4 as a functional read out parameter to assess flow deficits after ischemia. Active foot movement was significantly impaired in KO mice and restored in the presence of Dll4 vector or Dll4 vector in combination with Ang2. **(D)** Percentage of mice in each group presenting necrosis or amputation was determined. More KO mice had to be euthanized due to amputation or necrosis of the limb. Injection of Dll4 vector or Dll4 vector in combination with Ang2 significantly decreases necrosis and amputation. (Ctrl n=20, KO n=20) Data are means ± SEM. *P<0.05 and **P<0.01.